Linear and nonlinear solid-state optics

Temperature studies of optical absorption in the sandwich structure based on $(Ag_3AsS_3)_{0.6}(As_2S_3)_{0.4}$ thin film and gold nanoparticles

I.P. Studenyak[1,*], Z.R. Molnar[1], M.M. Kutsyk[1], V.Yu. Izai[1], M. Kranjčec[2], S. Kökényesi[3]

[1]*Uzhhorod National University, Faculty of Physics,*
3 Narodna Sq., 88000 Uzhhorod, Ukraine,

[2]*Department of Civil Engineering, University North,*
33 J. Križanića St., 642000 Varaždin, Croatia,

[3]*Department of Experimental Physics, Faculty of Science and Technology, University of Debrecen,*
18/a Bem Sq., 4026 Debrecen, Hungary,

[*] *E-mail: studenyak@dr.com*

Abstract. $(Ag_3AsS_3)_{0.6}(As_2S_3)_{0.4}$ thin films deposited using the thermal evaporation technique onto glass substrates previously covered with layers of gold nanoparticles were studied. Optical transmission spectra of the sandwich structure were studied within the temperature range 77–300 K. The absorption spectra in the region of its exponential behaviour were analyzed, the dispersion dependences of refractive index as well as the temperature dependences of the energy pseudogap and Urbach energy were investigated. The disordering processes in the sandwich structure were discussed. The comparative analyses of optical parameters in single $(Ag_3AsS_3)_{0.6}(As_2S_3)_{0.4}$ layer and in the sandwich structure were performed.

Keywords: thin film, gold nanoparticle, thermal evaporation, optical absorption, refractive index.

doi: https://doi.org/10.15407/spqeo21.01.089
PACS 78.40.Ha, 77.80.Bh

Manuscript received 27.02.10; revised version received 22.03.18; accepted for publication 29.03.18; published online 29.03.18.

1. Introduction

Among silver-containing chalcogenides, the Ag–As–S ternary system takes a remarkable place [1, 2]. Recently, we have reported about the structure [3], electrical conductivity [4], and optical absorption [5] in superionic Ag_3AsS_3–As_2S_3 glasses and composites. Thin films in this system, as in many other similar ones, were mainly prepared using deposition onto the substrates via vacuum deposition techniques, *i.e.*, thermal evaporation accompanied by a thermally or photo-induced dissolution of silver in As_2S_3 matrix [6, 7] or pulse laser deposition (PLD) [8]. Rather new method used is spin-coating technique [9, 10]. By the means of the PLD technique, a potentiometric thin film sensor can be realized on the basis of chalcogenide glasses (in particular, Ag–As–S) [11].

In Ref. [12], we presented the results of deposition of $(Ag_3AsS_3)_{0.6}(As_2S_3)_{0.4}$ thin films by rapid thermal evaporation in vacuum. SEM and AFM imaging the thin films revealed numerous micrometer-sized cones on their surfaces. The EDX analysis showed an excess of silver in the obtained cones, which, together with the pronounced peak of Ag in the XRD pattern, enabled us to ascribe the latter to the cones. It was shown that annealing and illumination lead to the increase of energy pseudogap, and to the decrease of refractive index. Additionally, it has been revealed that annealing and illumination cause the Urbach energy decrease and, respectively, the decrease of structural disordering in the $(Ag_3AsS_3)_{0.6}(As_2S_3)_{0.4}$ thin films [12].

Temperature behaviour of the absorption edge spectra for $(Ag_3AsS_3)_{0.6}(As_2S_3)_{0.4}$ thin film in the range of its exponential behaviour was studied in Ref. [13, 14]. A typical Urbach bundle was observed, temperature dependences of the energy pseudogap and Urbach energy were obtained. It was shown that the transition from the bulk composite to thin films was accompanied by a decrease of the coordinates of the Urbach bundle

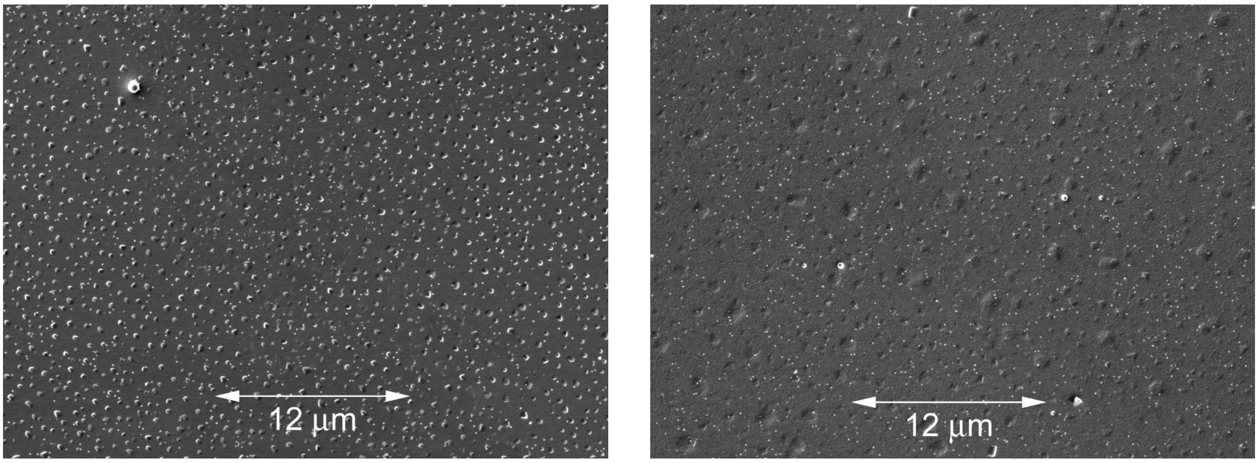

a b

Fig. 1. SEM images of the single layer $(Ag_3AsS_3)_{0.6}(As_2S_3)_{0.4}$ thin film (*a*) and sandwich structure with gold nanoparticles (*b*) prepared using RTE.

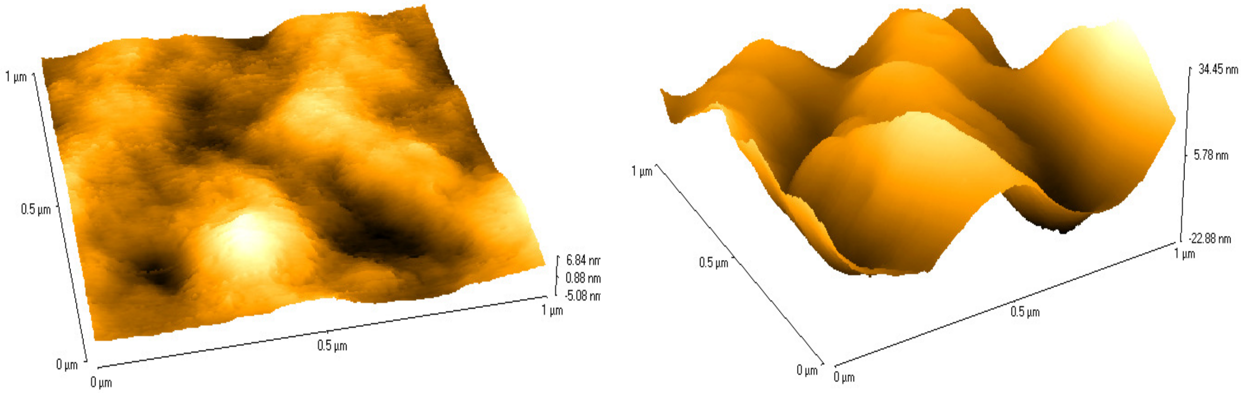

a b

Fig. 2. Three-dimensional AFM images of single layer $(Ag_3AsS_3)_{0.6}(As_2S_3)_{0.4}$ thin film (*a*) and sandwich structure with gold nanoparticles (*b*) prepared using RTE.

convergence point, a substantial enhancement of the electron-phonon interaction (EPI), an increase of the energy of effective phonon, taking part in the absorption edge formation, a significant increase of the Urbach energy as well as an increase of structural disordering. The analysis of compositional dependences of Urbach absorption edge parameters for $(Ag_3AsS_3)_x(As_2S_3)_{1-x}$ (x = 0.3, 0.6, 0.9) thin films was performed in Ref. [15].

The influence of laser and e-beam irradiation on structural and optical properties of $(Ag_3AsS_3)_{0.6}(As_2S_3)_{0.4}$ thin film was analyzed in Ref. [16]. Thin films were found to be sensitive to laser and e-beam irradiation, the latter can be used in all-optical switching devices as well as to improve optical recording.

In recent years, surface plasmon resonance has been used to enhance photostructural changes due to laser illumination [17]. Such surface plasmon resonance was revealed to influence the photoinduced transformations in chalcogenide As–S(Se) thin films [18]. Therefore, it was of a certain interest to obtain and examine these effects in new investigated Ag–As–S thin films. In this paper, we report on the temperature studies of optical absorption edge, investigations of temperature behaviour of the energy pseudogap, Urbach energy and refractive index as well as disordering processes in sandwich structure based on $(Ag_3AsS_3)_{0.6}(As_2S_3)_{0.4}$ thin film and gold nanoparticles (GNP).

2. Experimental

Synthesis of $(Ag_3AsS_3)_{0.6}(As_2S_3)_{0.4}$ composite material (which consists of crystalline Ag_3AsS_3 and glassy As_2S_3 [4]) was carried out at the temperature 700 °C for 24 h with subsequent melt homogenization for 72 h. Gold nanoparticles were obtained at the silica glass substrates by annealing of previously deposited using thermal evaporation thin films of gold [17]. Subsequently, the GNP layers were covered with the $(Ag_3AsS_3)_{0.6}(As_2S_3)_{0.4}$ thin films deposited using rapid thermal evaporation (RTE) from the corresponding material at the temperature 1350 °C in vacuum ($3\cdot10^{-3}$ Pa) with the VU-2M setup. The composite material was initially placed in a tantalum evaporator perforated for preventing the material falling out, on a glass substrate kept at room temperature.

Structural properties of the thin film and sandwich structure under investigations were studied using SEM and AFM. SEM and AFM images in Figs. 1 and 2 demonstrate the surface of thin film and sandwich structure. AFM measurements have shown the film with GNP to have higher mean roughness as compared to the $(Ag_3AsS_3)_{0.6}(As_2S_3)_{0.4}$ films without Au (Fig. 2). Energy-dispersive X-ray spectroscopy (EDX) within SEM was used to ensure thin films chemical composition.

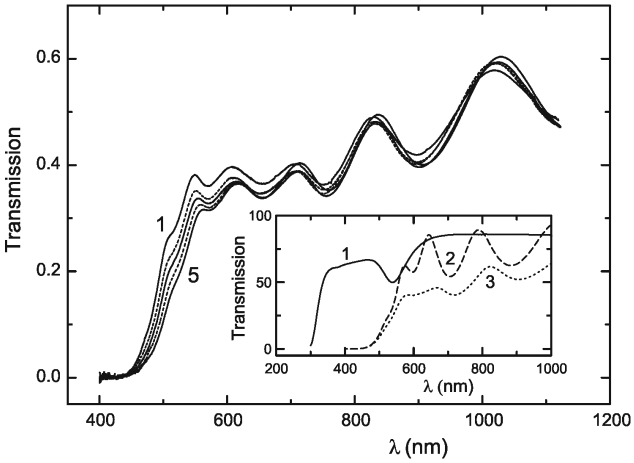

Fig. 3. Optical transmission spectra of the sandwich structure based on $Ag_3AsS_3)_{0.6}(As_2S_3)_{0.4}$ thin film and GNP at various temperatures: (*1*) 77, (*2*) 150, (*3*) 200, (*4*) 250, and (*5*) 300 K. The inset shows the optical transmission spectra of GNP nanoparticles (*1*), $(Ag_3AsS_3)_{0.6}(As_2S_3)_{0.4}$ thin film (*2*) and sandwich structure on their base (*3*).

The thickness of films was measured using the Ambios Stylus XP-1 profile meter. The thickness of $(Ag_3AsS_3)_{0.6}(As_2S_3)_{0.4}$ thin film was estimated to be 600 nm; initial GNP layers were obtained of 50-nm thickness.

Optical transmission spectra were studied in the interval of temperatures 77…300 K with the MDR-3 grating monochromator, a UTREX cryostat was used for low-temperature studies. From the temperature studies of interference transmission spectra, the spectral dependences of the absorption coefficient as well as the dispersion dependences of the refractive index were derived [19].

3. Results and discussion

Interferential transmission spectra of sandwich structure based on $(Ag_3AsS_3)_{0.6}(As_2S_3)_{0.4}$ thin film and GNP at various temperatures within the range 77–300 K are shown in Fig. 3. With temperature, a red shift of both the short-wave part of the transmission spectrum (related to the temperature behaviour of the absorption edge) and the interferential maxima are observed. Besides, a typical decrease of transmission in the interferential maxima with temperature is revealed. The inset to Fig. 3 demonstrates for comparison the transmission spectra of GNP nanoparticles, $(Ag_3AsS_3)_{0.6}(As_2S_3)_{0.4}$ thin film and sandwich structure on their base. It should be noted that the surface plasmon resonance of GNP was observed in the transmission spectra (Fig. 3). The most probably, the minimum in the spectrum of Au that corresponds to the plasmon resonance frequency of gold is shifted to the longer wavelengths in the sandwich structure, thus resulting in reduction of the transmittance peaks. This effect can be probably used in optical switching devices or can improve optical recording.

It is seen (Fig. 4) that the optical absorption edge spectra in the range of their exponential behaviour in the sandwich structure, similarly to $(Ag_3AsS_3)_{0.6}(As_2S_3)_{0.4}$ thin film [13, 14], are described by the Urbach rule [20]:

$$\alpha(h\nu,T)=\alpha_0\cdot\exp\left[\frac{\sigma(h\nu-E_0)}{kT}\right]=\alpha_0\cdot\exp\left[\frac{h\nu-E_0}{E_U(T)}\right], \quad (1)$$

where E_U is the Urbach energy (being reciprocal to the absorption edge slope $E_U^{-1}=\Delta(\ln\alpha)/\Delta(h\nu)$), σ – absorption edge steepness parameter, α_0 and E_0 are the convergence point coordinates of the Urbach bundle. The coordinates of the Urbach bundle convergence point α_0 and E_0 for the sandwich structure as well as for $(Ag_3AsS_3)_{0.6}(As_2S_3)_{0.4}$ thin film are given in Table.

Temperature behaviour of the Urbach absorption edge in the sandwich structure, similarly to $(Ag_3AsS_3)_{0.6}(As_2S_3)_{0.4}$ thin film [13, 14], is explained by electron-phonon interaction (EPI). The EPI parameters are obtained from the temperature dependence of absorption edge steepness parameter (Fig. 4) using the Mahr formula [21]:

$$\sigma(T)=\sigma_0\cdot\left(\frac{2kT}{\hbar\omega_p}\right)\cdot\tanh\left(\frac{\hbar\omega_p}{2kT}\right), \quad (2)$$

where $\hbar\omega_p$ is the effective phonon energy in the one-oscillator model describing the electron-phonon interaction, and σ_0 – parameter related to the EPI constant g as $\sigma_0=(2/3)g^{-1}$ (parameters $\hbar\omega_p$ and σ_0 are given in Table). For the sandwich structure as well as for $(Ag_3AsS_3)_{0.6}(As_2S_3)_{0.4}$ thin film, $\sigma_0 < 1$, which evidences for strong EPI [22]. Besides, in the sandwich structure, compared to the thin film, EPI is enhanced (it corresponds to a decrease of the σ_0 parameter) and the energy $\hbar\omega_p$ of effective phonon taking part in absorption edge formation decreases (Table).

It should be noted that, in the range of exponential behaviour of optical absorption edge for their spectral characterization, one can use the energy pseudogap E_g^α

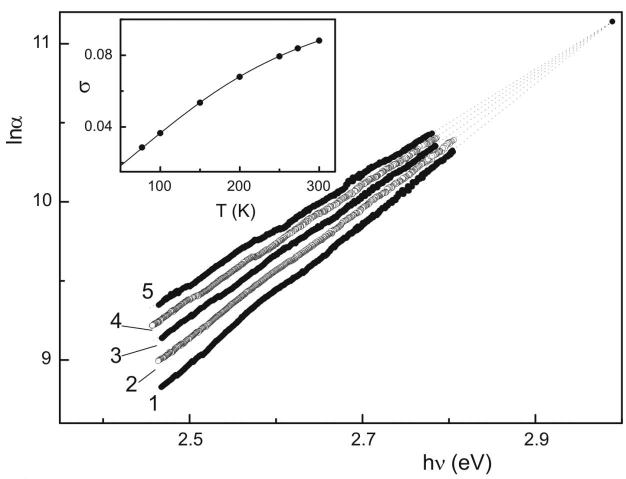

Fig. 4. Spectral dependences of the absorption coefficient of the sandwich structure based on $(Ag_3AsS_3)_{0.6}(As_2S_3)_{0.4}$ thin film and GNP at various temperatures: (*1*) 77, (*2*) 150, (*3*) 200, (*4*) 250, and (*5*) 300 K. The inset shows the temperature dependence of the steepness parameter σ.

Table. Parameters of the Urbach absorption edge and EPI for $(Ag_3AsS_3)_{0.6}(As_2S_3)_{0.4}$ thin film and sandwich structure with GNP prepared using RTE.

Material	$(Ag_3AsS_3)_{0.6}(As_2S_3)_{0.4}$ thin film	$(Ag_3AsS_3)_{0.6}(As_2S_3)_{0.4}$ thin film + GNP
α_0 (cm^{-1})	$1.5\cdot10^5$	$6.9\cdot10^4$
E_0 (eV)	2.756	2.990
E_g^α (eV)	2.465	2.895
E_U (meV)	272	297
σ_0	0.140	0.120
$\hbar\omega_p$ (meV)	63.1	56.2
θ_E (K)	732	652
$(E_U)_0$ (meV)	223	231
$(E_U)_1$ (meV)	507	513
$E_g^\alpha(0)$ (eV)	2.517	2.916
S_g^α	8.62	2.90

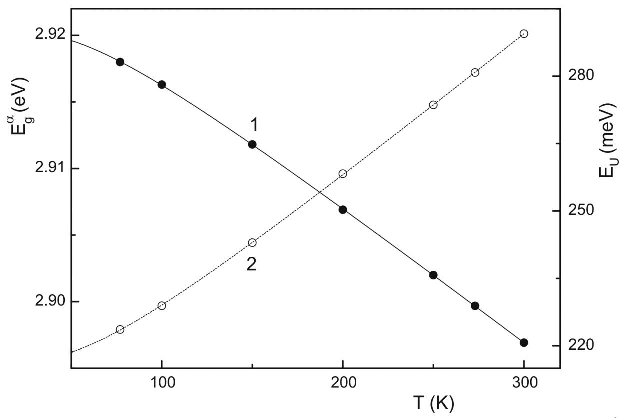

Fig. 5. Temperature dependences of the energy pseudogap E_g^α ($\alpha = 5\cdot10^4$ cm^{-1}) (*1*) and Urbach energy E_U (*2*) of the sandwich structure based on $Ag_3AsS_3)_{0.6}(As_2S_3)_{0.4}$ thin film and GNP.

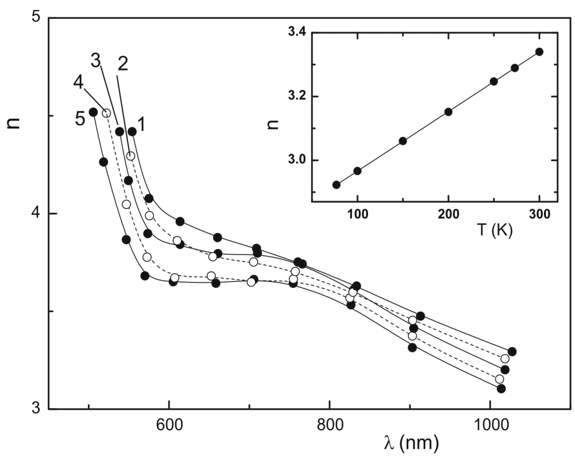

Fig. 6. Refractive index dispersion of the sandwich structure based on $Ag_3AsS_3)_{0.6}(As_2S_3)_{0.4}$ thin film and GNP at various temperatures: (*1*) 77, (*2*) 150, (*3*) 200, (*4*) 250, and (*5*) 300 K. The inset shows the temperature dependence of refractive index.

(E_g^α is the energy position of an exponential absorption edge at a fixed absorption coefficient α). Like to that in [12], we used the E_g^α values taken at $\alpha = 5\cdot10^4$ cm^{-1} for characterization of the absorption edge spectral position (Table). The temperature dependences of E_g^α and Urbach energy E_U for the sandwich structure are presented in Fig. 5 and can be described in the Einstein model by using the following relations [23, 24]

$$E_g^\alpha(T) = E_g^\alpha(0) - S_g^\alpha k\theta_E\left[\frac{1}{\exp(\theta_E/T)-1}\right], \qquad (3)$$

$$E_U(T) = (E_U)_0 + (E_U)_1\left[\frac{1}{\exp(\theta_E/T)-1}\right], \qquad (4)$$

where $E_g^\alpha(0)$ and S_g^α are the energy pseudogap at 0 K and a dimensionless constant, respectively; θ_E is the Einstein temperature, corresponding to the average frequency of phonon excitations of a system of non-coupled oscillators; $(E_U)_0$ and $(E_U)_1$ are constants. The obtained $E_g^\alpha(0)$, S_g^α, θ_E, $(E_U)_0$, and $(E_U)_1$ parameters for the sandwich structure as well as for $(Ag_3AsS_3)_{0.6}(As_2S_3)_{0.4}$ thin film are adduced in Table. The temperature dependences of E_g^α and Urbach energy E_U for the sandwich structure calculated from Eqs. (3) and (4) are shown in Fig. 4 as solid and dashed lines, respectively.

An essential characteristic of the absorption edge spectra of the sandwich structure as well as for $(Ag_3AsS_3)_{0.6}(As_2S_3)_{0.4}$ thin film are a lengthy Urbach tail, which results in the high value of the Urbach energy E_U (Table). In Ref. [25], it was shown that temperature, structural and compositional disordering affect the shape of Urbach absorption edge, *i.e.* the Urbach energy E_U is described by the following equation

$$E_U = (E_U)_T + (E_U)_X + (E_U)_C = (E_U)_T + (E_U)_{X+C}, \qquad (5)$$

where $(E_U)_T$, $(E_U)_X$, and $(E_U)_C$ are the contributions of temperature, structural and compositional disordering to E_U, respectively. It should be noted that the first term in the right-hand side of Eq. (4) represents the sum of structural and compositional disordering, and the second one represents temperature disordering. It is noteworthy that the absolute value of the contribution of structural disordering into the Urbach energy of the sandwich structure increases over than 9% in comparison with that of $(Ag_3AsS_3)_{0.6}(As_2S_3)_{0.4}$ thin film.

The dispersion dependences of the refractive index for the sandwich structure were obtained from the interference transmission spectra (Fig. 6). The slight dispersion of the refractive index is observed in the transparency region, while it increases when approaching to the optical absorption edge region. With increasing the temperature, the linear increase of refractive index in the sandwich structure has been revealed.

4. Conclusions

The sandwich structure based on $(Ag_3AsS_3)_{0.6}(As_2S_3)_{0.4}$ thin film and GNP were deposited onto a silica substrate by using rapid thermal evaporation. SEM imaging of the sandwich structure revealed numerous micrometer-sized Ag-containing cones on their surfaces. Temperature variation of the transmission spectra and the temperature behaviour of the absorption edge spectra within the range of its exponential behaviour for the sandwich structure were studied. The typical Urbach bundle has been observed, temperature dependences of the energy pseudogap and the Urbach energy have been obtained. The influence of different types of disordering on the Urbach tail of the sandwich structure has been studied. The dispersion dependences of the refractive index for the sandwich structure have been studied; with the temperature increase, the linear increase of refractive index in the sandwich structure has been revealed.

Finally, in the sandwich structure it can be observed: (1) the blue shift of the optical absorption edge and blenching of the sandwich structure compared to that in the $(Ag_3AsS_3)_{0.6}(As_2S_3)_{0.4}$ thin film; (2) the sandwich structure is more disordered than thin film, since the Urbach energy increases from 272 up to 297 meV (higher than 9%); (3) EPI enhances, and phonon energy decreases; (4) although the absolute value of statical structural disordering contribution into the Urbach energy slightly increases from 223 up to 231 meV (by 4%), however, the relative contribution insignificantly decreases from 82% to 78%.

References

1. Belford R.E., Hajto E., Owen A.E. The selective removal of the negative high-resolution photoresist system Ag-As-S. *Thin Solid Films*. 1989. **173**. P. 129–137.
2. Kozicki M.N., Mitkova M. Mass transport in chalcogenide electrolyte films – materials and applications. *J. Non-Cryst. Solids*. 2006. **352**. P. 567–577.
3. Studenyak I., Neimet Yu., Cserhati C., Kökényesi S., Kazakevičius E., Šalkus T., Kežionis A., Orliukas A. Structural and electrical investigations of $(Ag_3AsS_3)_x(As_2S_3)_{1-x}$ superionic glasses. *Cent. Eur. J. Phys.* 2012. **10**. P. 206–209.
4. Studenyak I.P., Neimet Yu.Yu., Kranjčec M., Solomon A.M., Orliukas A.F., Kežionis A., Kazakevičius E., Šalkus T. Electrical conductivity studies in $(Ag_3AsS_3)_x(As_2S_3)_{1-x}$ superionic glasses and composites. *J. Appl. Phys.* 2014. **115**. P. 033702-1–033702-5.
5. Studenyak I.P., Kranjčec M., Neimet Yu.Yu., Pop M.M. Optical absorption edge in $(Ag_3AsS_3)_x(As_2S_3)_{1-x}$ superionic glasses. *Semiconductor Physics, Quantum Electronics & Optoelectronics*. 2012. **15**. P. 147–151.
6. Wagner T., Perina V., Mackov A., Rauhala E., Seppala A., Vlcek Mir., Kasap S.O., Vlcek Mil., Frumar M. The tailoring of the composition of Ag–As–S amorphous films using photo-induced solid state reaction between Ag and $As_{30}S_{70}$ films. *Solid State Ionics*. 2001. **141–142**. P. 387–395.
7. Kovalskiy A., Jain H., Mitkova M. Evolution of chemical structure during silver photodiffusion into chalcogenide glass thin films. *J. Non-Cryst. Solids*. 2009. **355**. P. 1924–1929.
8. Nemec P., Frumar M., Jedelsky J., Jelınek M., Lancok J., Gregora I. Thin amorphous chalcogenide films prepared by pulsed laser deposition. *J. Non-Cryst. Solids*. 2002. **299–302**. P. 1013–1017.
9. Wagner T., Kohoutek T., Vlcek Mir., Vlcek Mil., Munzar M., Frumar M. Spin-coated $Ag_x(As_{0.33}S_{0.67})_{100-x}$ films: preparation and structure. *J. Non-Cryst. Solids*. 2003. **326–327**. P. 165–169.
10. Kohoutek T., Wagner T., Orava J., Frumar M., Perina V., Mackova A., Hnatowitz V., Vlcek M., Kasap S. Amorphous films of Ag–As–S system prepared by spin-coating technique, preparation techniques and films physico-chemical properties. *Vacuum*. 2004. **76**. P. 191–194.
11. Schoening M.J., Schmidt C., Schubert J., Zander W., Mesters S., Kordos P., Lueth H., Legin A., Seleznev B., Vlasov Yu.G. Thin films on the basis of chalcogenide glass materials prepared by pulsed laser deposition technique. *Sensors and Actuators B*. 2000. **68**. P. 254–259.
12. Studenyak I.P., Neimet Yu.Yu., Rati Y.Y., Stanko D., Kranjčec M., Kökényesi S., Daróci L., Bohdan R. Structural and optical properties of annealed and illuminated $(Ag_3AsS_3)_{0.6}(As_2S_3)_{0.4}$ thin films. *Opt. Mat*. 2014. **37**. P. 718–723.
13. Studenyak I.P., Kutsyk M.M., Rati Y.Y., Izai V.Yu., Kökényesi S., Daróci L., Bohdan R. Temperature studies of optical parameters in $(Ag_3AsS_3)_{0.6}(As_2S_3)_{0.4}$ thin films. *Semiconductor Physics, Quantum Electronics & Optoelectronics*. 2015. **18**. P. 188–192.
14. Studenyak I.P., Kutsyk M.M., Buchuk M.Yu., Rati Y.Y., Neimet Yu.Yu., Izai V.Yu., Kökényesi S., Nemec P. Temperature studies of optical parameters of $(Ag_3AsS_3)_{0.6}(As_2S_3)_{0.4}$ thin films prepared by rapid thermal evaporation and pulse laser deposition. *Opt. Mat*. 2016. **52**. P. 224–229.
15. Studenyak I.P., Kranjčec M., Kutsyk M.M., Pal Yu.O., Neimet Yu.Yu., Izai V.Yu., Makauz I.I., Cserhati C., Kökényesi S. Compositional studies of optical parameters in $(Ag_3AsS_3)_x(As_2S_3)_{1-x}$ (x = 0.3; 0.6; 0.9) thin films. *Semiconductor Physics, Quantum Electronics & Optoelectronics*. 2016. **19**. P. 371–376.
16. Neimet Yu.Yu., Studenyak I.P., Buchuk M.Yu., Bohdan R., Kökényesi S., Daróci L., Nemec P. Photo-induced effects in $(Ag_3AsS_3)_{0.6}(As_2S_3)_{0.4}$ thin films and multilayers with gold nanoparticles. *Semiconductor Physics, Quantum Electronics & Optoelectronics*. 2015. **18**. P. 385–390.
17. Charnovych S., Kökényesi S., Glodan Gy., Csik A. Enhancement of photoinduced transformations in

amorphous chalcogenide film via surface plasmon resonances. *Thin Solid Films*. 2011. **519**. P. 4309–4312.
18. Charnovych S., Dmitruk N., Yurkovich N., Shiplyak M., Kokenyesi S. Photo-induced changes in a-As_2S_3/gold nanoparticle composite layer structures. *Thin Solid Films*. 2013. **548**. P. 419–424.
19. Swanepoel R. Determination of the thickness and optical constants of amorphous silicon. *J. Phys. E: Sci. Instrum*. 1983. **16**. P. 1214–1222.
20. Urbach F. The long-wavelength edge of photographic sensitivity and of the electronic absorption of solids. *Phys. Rev*. 1953. **92**. P. 1324–1326.
21. Sumi H., Sumi A. The Urbach–Martienssen rule revisited. *J. Phys. Soc. Jpn*. 1987. **56**. P. 2211–2220.
22. Kurik M.V. Urbach rule (Review). *phys. status solidi* (*a*). 1971. **8**. P. 9–30.
23. Beaudoin M., DeVries A.J.G., Johnson S.R., Laman H., Tiedje T. Optical absorption edge of semi-insulating GaAs and InP at high temperatures. *Appl. Phys. Lett*. 1997. **70**. P. 3540–3542.
24. Yang Z., Homewood K.P., Finney M.S., Harry M.A., Reeson K.J. Optical absorption study of ion beam synthesized polycrystalline semiconducting $FeSi_2$. *J. Appl. Phys*. 1995. **78**. P. 1958–1963.
25. Cody G.D., Tiedje T., Abeles B., Brooks B., Goldstein Y., Disorder and the optical-absorption edge of hydrogenated amorphous silicon. *Phys. Rev. Lett*. 1981. **47**. P. 1480–1483.

Authors and CV

Studenyak I.P.: Doctor of Physical and Mathematical Sciences, Professor, Vice-rector for Research at Uzhhorod National University. The area of scientific interests is physical properties of semiconductors, ferroics and superionic conductors.
Uzhhorod National University, Faculty of Physics
E-mail: studenyak@dr.com

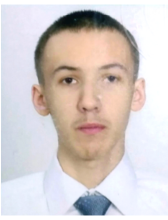

Molnar Z.R.: Student of Physics Faculty at Uzhhorod National University. The area of scientific interests is structural and optical parameters of solids.
Uzhhorod National University, Faculty of Physics

Kutsyk M.M.: Component Engineer at Flex Ltd (Mukachevo, Ukraine). The area of scientific interests is optical parameters of solids.
Uzhhorod National University, Faculty of Physics

Izai V.Yu.: Ph.D, Senior Researcher at Uzhhorod National University. The area of scientific interests is electrical and optical properties of superionic conductors.
Uzhhorod National University, Faculty of Physics

Kranjčec M.: Ph.D, Professor at University North (Varaždin, Croatia). The area of scientific interests is optical properties of semiconductors.
Department of Civil Engineering, University North

Kökényesi S.: Doctor of Physical and Mathematical Sciences, Professor at University of Debrecen (Hungary). The area of scientific interests is physical properties of amorphous semiconductors.
Department of Experimental Physics, Faculty of Science and Technology, University of Debrecen